Inorganic Chemistry

ARTICLE

pubs.acs.org/IC

Metallophilic Bonding and Agostic Interactions in Gold(I) and Silver(I) Complexes Bearing a Thiotetrazole Unit

Adriana Ilie,[†,‡] Ciprian I. Raţ,[‡] Susanne Scheutzow,[†] Christiane Kiske,[†] Karin Lux,[†] Thomas M. Klapötke,[†] Cristian Silvestru,[‡] and Konstantin Karaghiosoff*,[†]

[†]Department of Chemistry, Ludwig-Maximilians-University Butenandtstrasse. 5-13 (Haus D), Munich, D-81377, Grosshadern, Germany

[‡]Faculty of Chemistry & Chemical Engineering, Babes-Bolyai University, Arany Janos str. No. 11, 400028, Cluj-Napoca, Romania

Supporting Information

ABSTRACT: Gold(I) and silver(I) complexes of 1-methyl-5-thio-tetrazole (**1**) have been prepared and the coordination chemistry of this ligand toward metal-phosphine frameworks has been explored. As indicated by IR and Raman data, ligand **1** is deprotonated and the resulted anion acts as a bidentate (*S,N*)-tetrazole-5-thiolato unit in the new gold(I) complexes, [Au(SCN_4Me)(PPh_3)] (**2**), [{Au(SCN_4Me)}$_2$(μ-dppm)] (**3**), and [{Au(SCN_4Me)}$_2$(μ-dppe)] (**4**), while it is coordinated only through the sulfur atom as its neutral tetrazole-5-thione form in the silver(I) derivative, [Ag($HSCN_4Me$)(PPh_3)]$_2$(OTf)$_2$ (**5**). Further characterization of the new compounds was performed using multinuclear (^1H, ^{13}C, ^{31}P, ^{19}F) NMR spectroscopy, mass spectrometry, and DSC measurements. Single-crystal X-ray diffraction studies revealed basically linear P-M-S arrangements in complexes **3**−**5**. The bidentate (*S,N*) coordination pattern results in a T-shaped (*S,N*)PAu core in **3** and **4**, whereas, in **5**, a similar coordination geometry is achieved in the dimer association based on *S*-bridging ligand **1**. Herein, weak (C)H···Au and (C)H···Ag agostic interactions were observed. An intramolecular Au···Au contact occurs in **3**, while in **4** intermolecular aurophilic bonds lead to formation of a chain polymer. An intermolecular Ag···Ag contact is also present in the dimer unit of **5**. Low-temperature ^{31}P NMR data for **5** evidenced the presence of monomer and dimer units in solution. Theoretical calculations on model of the complexes **2** and **4** are consistent with the geometries found by X-ray diffraction studies.

1. INTRODUCTION

Complexes bearing the M−S (M = Au, Ag) bond have raised continuously increasing interest, because of their use in pharmacology[1] and thin films,[2] as well as glass and ceramic technology.[3] A variety of heterocyclic ligands have been used to study their complexation abilities with heavy metals,[4] and, among them, thiotetrazoles have proved to be promising ligands. Their relative stability to oxidation and high coordination ability[5] lead to applications in photothermographic and photographic materials,[6] or use as capping agents for the stabilization of gold nanoparticles.[7] However, research on coordination chemistry of thiotetrazoles toward gold and silver has been scarcely reported. The first Au(I) and Ag(I) complexes with thiotetrazoles, i.e., [M($HSCN_4R$)] [M = Au(I), Ag(I); R = Ph, 1-MeOC_6H_4, 3-ClC_6H_4, 2-MeC_6H_4],[8] were synthesized by Agarwala et al., while Beck et al. managed to also incorporate phosphine fragments, e.g., [Au(SCN_4R)(PPh_3)] (R = Me, Ph) and [Ag(SCN_4R)(PPh_3)$_2$].[9] In such gold(I) complexes,[9] aurophilicity (the affinity between gold atoms)[10] was noted. The structures of the first ionic Au(III) compounds with monodentate tetrazole-5-thiolato ligands, e.g., [{(2-Me_2HNCH_2)C_6H_4}Au(SCN_4Me)$_3$], [PPh_4][Au(SCN_4Me)$_4$]·0.5H_2O, were also reported by Abram et al.[11]

In this context, we set out to design, prepare, and characterize gold(I) and silver(I) complexes of 1-methyl-5-thio-tetrazole (**1**), using different phosphine-metal moieties and taking into account the coordination versatility of the thio ligand. A single-crystal X-ray diffraction (XRD) study revealed the thione nature of **1** in the solid state.[12] The coordination chemistry of thiotetrazoles, including **1**, toward metal atoms is strongly related to their thiol (**1a**, 1-methyl-1*H*-tetrazole-5-thiol) or thione [**1b**, 1-methyl-1*H*-tetrazole-5(4*H*)-thione] tautomers (see Figure 1). As a consequence, **1** can act as neutral ligand bound to a metal atom through the sulfur atom of the thione tautomer (**A**) or as a monoanionic ligand bound to the metal either through a nitrogen atom (**B**, deprotonated **1b**) or a sulfur atom (**C**, deprotonated **1a**) (see Figure 1).

2. RESULTS AND DISCUSSION

Ligand **1** was prepared following a straightforward strategy.[13] The synthetic route for the preparation of [Au(SCN_4Me)(PPh_3)] (**2**) differs from the strategy used by Beck et al.[9] Thus, **2** was obtained in high yields from equimolar amounts of **1** and the precursor [AuCl(PPh_3)], using THF as a solvent. The reaction of **1** with [Au_2Cl_2(μ-dppm)] (dppm = $Ph_2PCH_2PPh_2$) or [Au_2Cl_2(μ-dppe)] (dppe = $Ph_2PCH_2CH_2PPh_2$), respectively, in 2:1 molar ratio, yielded the target compounds [{Au(SCN_4Me)}$_2$(μ-dppm)] (**3**) and [{Au(SCN_4Me)}$_2$(μ-dppe)] (**4**) (Scheme 1). These synthetic procedures required the use of NEt_3 as a base to trap the resulting HCl. Complex [Ag($HSCN_4$

Received: December 31, 2010
Published: February 10, 2011

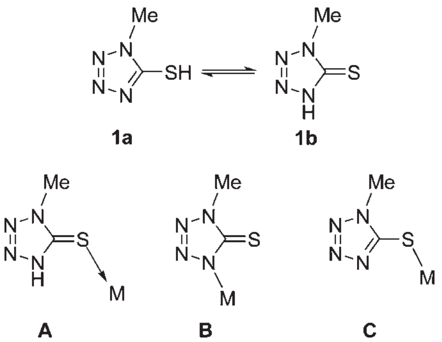

Figure 1. Thiol and thione tautomers for thiotetrazole 1 and coordination patterns toward a metal atom.

Scheme 1. Synthesis of Complexes 2−5. [a]

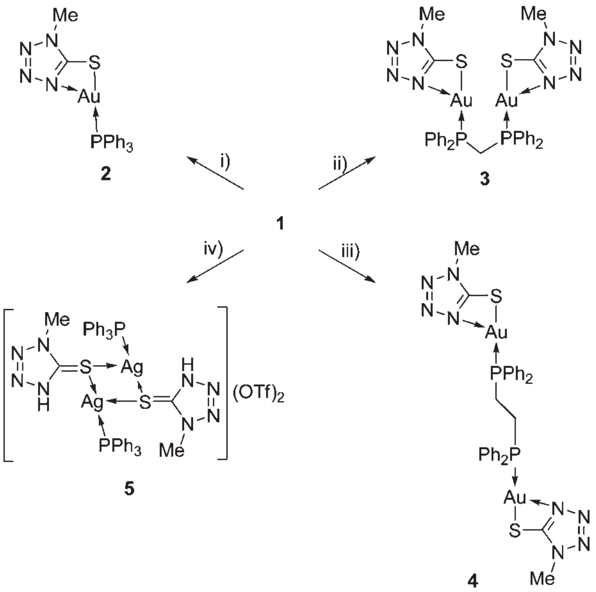

[a] Reagents and conditions: (i) [AuCl(PPh_3)], THF, Et_3N, r.t., 80%; (ii) [Au_2Cl_2(μ-dppm)], THF, Et_3N, r.t., 91%; (iii) [Au_2Cl_2(μ-dppe)], THF, Et_3N, r.t., 81%; and (iv) [Ag(OTf)(PPh_3)], CH_2Cl_2, r.t. 85%.

Me)(PPh_3)]$_2$(OTf)$_2$ (**5**) was prepared from **1** and [Ag(OTf)(PPh_3)], in 1:1 molar ratio, using CH_2Cl_2 as a solvent.

The ^{1}H NMR studies revealed several diagnostic characteristics. Compared to the free ligand **1**, new resonances (i.e., a triplet at δ = 3.7 ppm and a broad singlet at δ = 3.1 ppm) appear for complexes **3** and **4**, respectively, and were assigned to methylene and ethylene protons in the diphosphine moieties. At a first glance, the ^{13}C NMR spectra of **2**, **3**, and **5** exhibit the expected resonances. For the carbon of the tetrazole ring, an upfield shift was noted, with respect to the free ligand ($\Delta\delta$ = 5.92 ppm in **2**, $\Delta\delta$ = 5.75 ppm in **3**, $\Delta\delta$ = 2.61 ppm in **5**), which is indicative for the formation of the complexes. For **3**, the aromatic carbons gave triplet resonances due to geminal and long-range phosphorus−carbon coupling systems. In the aromatic region of **2** and **5**, the ^{31}P−^{13}C couplings resulted in doublet resonances. The ^{31}P NMR spectra of complexes **2**−**4**, measured at room temperature in $CDCl_3$, showed one resonance at δ = 37.8 (**2**), 30.9 (**3**), and 38.3 ppm (**4**), respectively, the chemical shifts being in the usual region for the corresponding phosphorus ligands coordinated to Au(I).

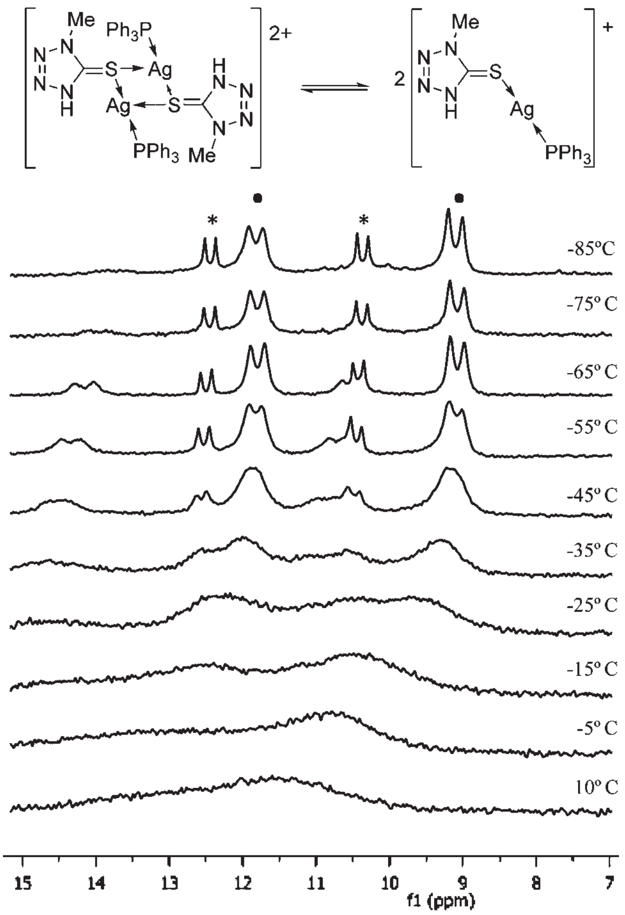

Figure 2. Variable-temperature ^{31}P NMR spectra of a solution of **5** in CD_2Cl_2. The marked signals correspond to dimer (*) and monomer (●).

For the silver complex **5**, the ^{31}P NMR spectrum, recorded at room temperature, exhibits a broad resonance in the δ range of 11−12 ppm, probably because of dissociative processes involving cleavage of S-AgPPh_3 and/or Ag-PPh_3 bonds, observation well-documented in case of phosphine complexes in the case of phosphine complexes of coinage metals.[14] Given these results, variable-temperature NMR studies in solution were performed (Figure 2). At low temperature (−85 °C), the ^{31}P NMR spectrum recorded in CD_2Cl_2 shows the presence of two resonances, each of them with a pattern of doublet of doublets due to the couplings with ^{107}Ag and ^{109}Ag isotopes, thus indicating the presence of two species containing silver−phosphine moieties which were assumed to be a monomer and a dimer species.

The coordination number (CN) around a silver atom in a silver−phosphine species can be estimated on the basis of the magnitude of the silver−phosphorus coupling constant. Thus, it was reported that the ^{1}J(P,^{107}Ag) coupling constants are inversely proportional to the coordination number of the silver atom[15] and increase with decreasing Ag−P distances.[16] Hence, the observed coupling constants for **5** may be assigned to the monomer (^{1}J(P,^{107}Ag) of 417.5 Hz, CN = 2) and dimer (^{1}J(P,^{107}Ag) of 318.5 Hz, CN = 3) species, respectively. The intensity of the signals suggests that the monomer is the predominant species in solution at lower temperatures. On the basis of the ^{31}P NMR investigations, it can be concluded that, in a

dx.doi.org/10.1021/ic102595d |Inorg. Chem. 2011, 50, 2675–2684

solution of **5**, there is an equilibrium between monomer and dimer units.

During the ES-MS analyses of gold(I) complexes **2**, **3**, and **4**, the formation of several gold species was observed. The ES-MS of **2** shows the molecular peak at m/z = 575.3 $[M+H]^+$ and a peak at m/z = 721.4, because of the monocharged species $[Au(PPh_3)_2]^+$. A different fragmentation pattern was noticed in the case of **3** and **4**, which lose the thiotetrazole fragment under the ionization conditions of ES-MS. The mass spectrum of **3** exhibits the main peak at m/z = 893.1 assigned to the fragment $[Au_2(SCN_4Me)(\mu\text{-dppm})]^+$, whereas, in **4**, along with $[Au_2(SCN_4Me)(\mu\text{-dppe})]^+$ fragment at m/z = 907.1, a lower mass fragment at m/z = 824.1 is due to the loss of the second thiotetrazole unit. The ES-MS of **5** exhibits the base peak at 631.2, corresponding to a $[Ag(PPh_3)_2]^+$ fragment.

Comparative analysis of IR and Raman spectra of ligand **1** with those of complexes **2**−**5** confirmed the formation of the metal−sulfur species. The characteristic bands of the ligand **1**,[8a,17] i.e., ν(N−C═S) at 1506 cm^{-1} and ν(C═S) at 1349, 1043, and 781 cm^{-1}, disappear in **2**−**4**. However, the appearance of a new split band at 711/692 cm^{-1} for **2**, 704/688 cm^{-1} for **3**, and 702/698 cm^{-1} for **4**, because of the contributions from the ν(C−S) stretching vibration, suggests the presence of the deprotonated **1** as a thiolato moiety attached to the gold center (pattern C, Figure 1). The C═S stretching frequencies are observed for **5** and shift downward to ~1337, 1014, and 750 cm^{-1}, because of coordination. This observation underlines that **1** is coordinated as its thione tautomer in **5**. The bidentate (*S*,*N*) coordination pattern of the thiolato moiety to gold is clearly indicated in the Raman spectra of **2**−**4**, where the ν(Au−N) vibrations[18] were located at 432 cm^{-1} in **2** and 438 cm^{-1} in **3** and **4**. For **5**, no band could be assigned to the ν(Ag−N) vibration. In the region of 340−450 cm^{-1}, which is characteristic for vibrations of the metal−sulfur bonds, a band, which is not present in the spectrum of the free ligand, appears in the spectra of the complexes and it was assigned to ν(M-S) vibration: 346 cm^{-1} in **2**, 343 cm^{-1} in **3**, 339 cm^{-1} in **4** (M = Au), and 350 cm^{-1} in **5** (M = Ag).

The thermal stability of **2**−**5** was determined using DSC measurements. The DSC revealed high thermal stabilities with high exothermic decompositions. Compound **2** melts at 154 °C and decomposes at 218 °C. For compounds **3** and **4**, only the decomposition points were observed at 247 and 255 °C, respectively. By contrast, the silver complex **5** with a melting point at 159 °C has two decomposition points, which were observed at 209 and 280 °C, respectively.

The structure of complexes **3** and **4** was established by X-ray diffraction (XRD) studies. Single crystals were obtained from methylene chloride/diethyl ether (1:4 by volume) by slow diffusion at room temperature (for **3** and **4**) or by slow evaporation of a methylene chloride solution (for **5**). The crystal structure of **3** contains two independent molecules and, therefore, subsequent discussion at the molecular level will refer to molecules **3a** and **3b** (see Figure 3).

In both molecules, the gold atoms are dicoordinated with an almost-linear S−Au−P fragment [P(1)−Au(1)−S(1), 173.05(5)°; P(2)−Au(2)−S(2), 176.74(5)° in **3a**; P(3)−Au(3)−S(3), 169.13(5)°; P(4)−Au(4)−S(4), 173.03(5)° in **3b**]. Intramolecular Au···Au (aurophilic) interactions were observed in both cases and they are likely to induce the deviation from linearity of the S−Au−P systems. The Au−Au distance in the molecules of **3** are significantly different: Au(1)···Au(2), 3.2142(3) Å in **3a**, and Au(3)···Au(4), 3.1046(3) Å in **3b** [cf.

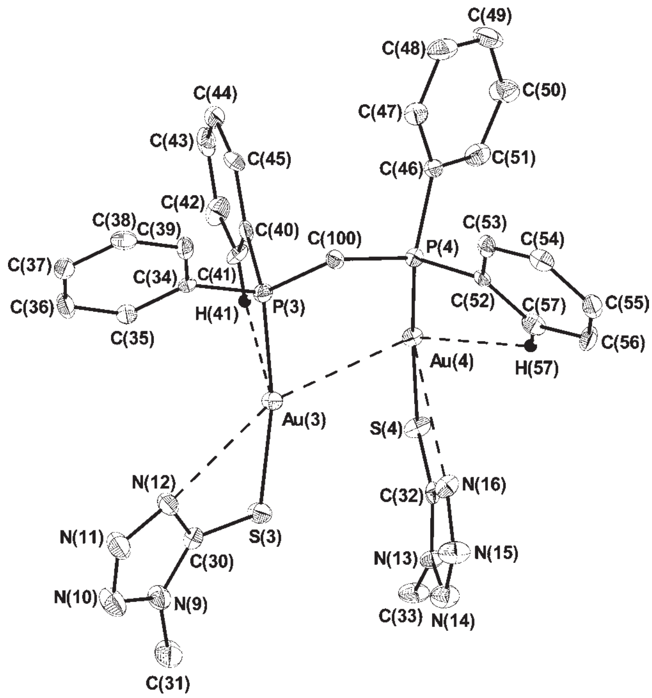

Figure 3. Structure of molecule **3b**, showing the atom numbering scheme. Displacement ellipsoids are depicted at the 50% probability level. Hydrogen atoms (except those involved in agostic interactions) are omitted for the sake of clarity. Selected bonds lengths (Å): Au(3)···Au(4), 3.1046(3); Au(3)−S(3), 2.3277(14); Au(4)−S(4), 2.3207(13); Au(3)−P(3), 2.2531(14); Au(4)−P(4), 2.2608(13); Au(3)−N(12), 3.146(5); Au(4)−N(16), 3.113(5); C(41)···Au(3), 3.429(6); H(41)···Au(3), 2.82; C(57)···Au(4), 3.410(5); H(57)···Au(4), 2.82; Au(3)−S(3), 2.3277(14); Au(4)−S(4), 2.3207(13); S(3)−C(30), 1.749(5); and S(4)−C(32), 1.737(5); angles (degrees): P(3)−Au(3)−S(3), 169.13(5); P(4)−Au(4)−S(4), 173.03(5); Au(3)−N(12)−C(30), 75.45(3); Au(4)−N(16)−C(32), 75.73(3); C(41)−H(41)···Au(3), 123.3(4); and C(57)−H(57)···Au(4), 121.5(3).

sum of the covalent and van der Waals radii, $\sum r_{cov}$(Au,Au) = 2.68 Å, $\sum r_{vdW}$(Au,Au) = 3.4 Å].[19] Also note that the nitrogen atoms are weakly coordinated to the gold atoms in **3b** [Au(3)−N(12), 3.146(5) Å; Au(4)−N(16), 3.113(5) Å], while in **3a**, no intramolecular N → Au interaction is present [the shortest nonbonding gold−nitrogen distances are Au(1)···N(4), 3.342(5) Å; Au(2)···N(8), 3.281(4) Å; cf. $\sum r_{vdW}$(Au,N) = 3.25 Å].[19] If intramolecular N → Au interactions are taken into account the coordination number of the gold atoms is increased to three in molecule **3b** and the coordination geometry can be described as T-shaped, whereas in **3a**, the gold atoms remain dicoordinated.

The presence of (C)H···Au[20] and (C)H···Ag[21] agostic interactions have not received much attention so far. For all complexes discussed in this work, such interactions were observed. Thus, in **3a** and **3b**, there are agostic intramolecular (C)H···Au interactions that involve aromatic hydrogen atoms in their calculated position[20h] [H(12)···Au(1) 2.94 Å and H(29)···Au(2) 2.99 Å in **3a**; H(41)···Au(3), 2.82 Å and H(57)···Au(4), 2.82 Å in **3b**; cf. $\sum r_{vdW}$(Au,H) = 3.15 Å].[19]

The crystal of the related complex **4** contains three independent molecules: **4a**, **4b**, and **4c**. The tetrazole-5-thiolato ligand is coordinated through sulfur to the gold center, resulting in an

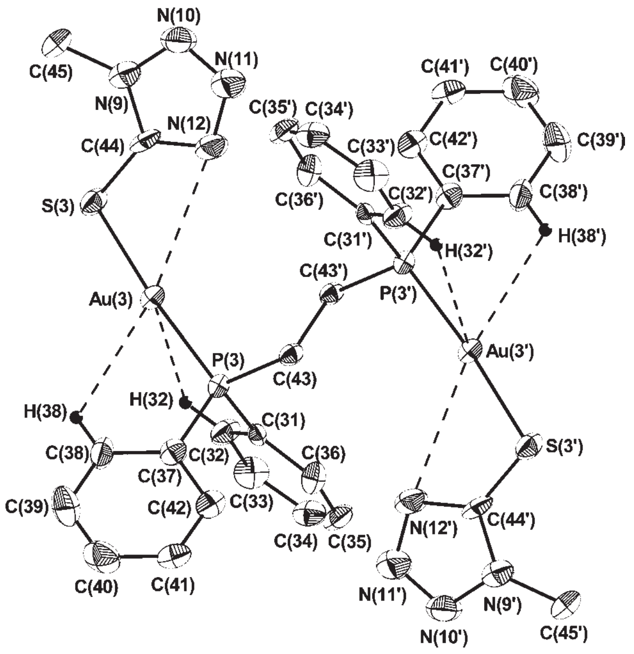

Figure 4. Structure of molecule **4c**, showing the atom numbering scheme. Displacement ellipsoids are depicted at the 50% probability level. Hydrogen atoms (except those involved in agostic interactions) are omitted for the sake of clarity. Selected bonds lengths (Å): Au(3)−S(3), 2.3214(16); Au(3)−P(3), 2.2487(16); Au(3)−N(12), 3.111(9); C(32)···Au(3), 3.460(6); H(32)···Au(3), 2.91; C(38)···Au(3), 3.58(1); H(38)···Au(3), 3.01; S(3)−C(44), 1.705(8); P(3)−C(43), 1.838(6); P(3)−C(31), 1.809(6); P(3)−C(37), 1.809(6); angles (°): P(3)−Au(3)−S(3), 174.76(6); Au(3)−S(3)−C(44), 95.2(2); C(32)−H(32)···Au(3), 118.4(4); C(38)−H(38)···Au(3), 120.4(5); Au(3)−P(3)−C(31), 110.7(2); Au(3)−P(3)−C(37), 116.3(2); and Au(3)−P(3)−C(43), 112.27(18).

almost-linear P−Au−S arrangement, ranging from 173.41(7)° in **4b** and 174.76(6)° in **4c** (see Figure 4) to 175.19(6)° in **4a**.

The coordination sphere of Au is accomplished in **4c** via an N→Au interaction [N(12)−Au(3), 3.111(9) Å], therefore the coordination geometry around Au(I) can be described as T-shaped. Two agostic interactions [H(32)···Au(3), 2.91 Å; H(38)···Au(3), 3.01 Å] per gold atom are also present. By contrast, in molecules **4a** and **4b**, no intramolecular N → Au interaction was observed [nonbonding N···Au, 3.293(6) Å in **4a** and 3.390(7) Å in **4b**]; however, **4a** is stabilized by (C)H···Au contacts [H(2)···Au(1), 2.94 Å; H(13′A)···Au(1), 2.95 Å]. (See the Supporting Information.) The agostic interaction with a distance of ca. 2.8 Å can be considered to be fairly weak,[20f] but they provide additional stabilization for **3a**, **3b**, **4a**, and **4c** and strengthen their overall geometry. The (C)H···Au distances observed for complexes **3** and **4** are in the middle of the range of agostic interactions previously reported for gold(I) complexes.[20c−20g]

The Au−S bond lengths in **3a** [Au(1)−S(1), 2.3322(14) Å; Au(2)−S(2), 2.3210(14) Å], **3b** [Au(3)−S(3), 2.3277(14) Å; Au(4)−S(4), 2.3207(13) Å], **4a** [Au(1)−S(1), 2.3444(17) Å], **4b** [Au(2)−S(2), 2.3256(15) Å], and **4c** [Au(3)−S(3), 2.3214(16) Å], respectively, are in the range reported for gold thiolato and thionato complexes.[22] It is worth mentioning that, in **3** and **4**, the carbon−sulfur bond distances do not resemble the value measured for the free ligand **1** [1.677(1) Å], being considerably longer [1.741(5)/1.739(6) Å in **3a**, 1.749(5)/1.737(5) Å in **3b**, 1.746(7) in **4a**, 1.720(6) in **4b**, and 1.705(8) in **4c**]. This indicates that the ligand is coordinated in the thiolato form. The magnitude of the Au−P distances [2.2529(14) Å, 2.2603(14) Å in **3a**, 2.2531(14) Å, 2.2608(13) Å in **3b**, 2.2618(17) Å in **4a**, 2.2577(15) Å in **4b**, and 2.2487(16) Å in **4c**] compares well with those found in the starting materials [Au_2Cl_2(μ-dppm)] [2.2384(15) Å] and [Au_2Cl_2(μ-dppe)] [2.2305(30) Å, 2.2289(36) Å], respectively. In contrast to **3**, the molecules of **4** do not exhibit intramolecular Au−Au interactions [the nonbonding Au···Au distances are in the range of 6.7038(6)−6.8977(6) Å]. This behavior is due to the *trans* arrangement of the AuSR fragments, with respect to the P−C−C-P skeleton. However, intermolecular Au−Au short contacts are observed [Au(1′)···Au(2), 3.1038(4)Å] between molecules **4a** and **4b**, because of the low coordination number and linear geometry of gold(I), which were found to be an excellent basis for the construction of one-dimensional polymers with gold atoms at regular intervals (see Figure 5). The Au(1′)···Au(2) distance resemble the values found in the literature for gold(I) complexes.[23] Moreover, the polymeric chain is stabilized through weak intermolecular (C)H···Au agostic interactions [H(8′)···Au(2), 2.84 Å]. In addition, weak intermolecular S···Au interactions are also established between molecules **4a** and **4b**, i.e., S(1′)···Au(2), 3.3821(19) Å,; S(2)···Au(1′), 3.4370(16) Å [c.f. $\sum r_{\mathrm{vdW}}$(S,Au) = 3.55 Å][19] (Figure 5). Molecule **4c**, because of the intramolecular N → Au coordination, is not involved in any Au−Au intermolecular interaction. Moreover, the sulfur atoms in **4c** remain free of any intermolecular contacts with gold atoms.

Single-crystal XRD analysis revealed that the crystal of **5** contains dinuclear dications (Figure 6). The carbon−sulfur bonds [S(2)−C(39), 1.689(5) Å; and S(1)−C(37), 1.687(6) Å] in **5** are rather small when compared to the corresponding bonds found in **3** and **4**, thus suggesting that ligand **1** coordinates to silver center in the thione form. The asymmetric bridging sulfur atoms from thione tautomers of ligand **1** generate a strictly planar, rhombic Ag_2S_2 core [Ag(1)−S(2), 2.4802(17) Å; Ag(1)···S(1), 2.9434(15) Å; Ag(2)−S(1), 2.4632(16) Å; Ag(2)···S(2), 2.9305(15) Å] [c.f. $\sum r_{\mathrm{cov}}$(Ag,S) = 2.38 Å, $\sum r_{\mathrm{vdW}}$(Ag,S) = 3.55 Å].[19] The endocyclic bond angles (i.e., S(1)−Ag(1)−S(2)/S(1)−Ag(2)−S(2), 112.03(5)/112.98(5)°; Ag(1)−S(1)−Ag(2)/Ag(1)−S(2)−Ag(2), 67.46(4)/67.49(4)°) differ considerably from those found in other sulfur-bridged species containing Ag(I).[24] The formation of the dimer in the solid state is achieved because of the strength of the Ag···S interactions between the two mononuclear units. This is supported by literature data on Ag−S bonds and contacts[24,25] and also suggests that the weaker Ag···S distances are probably the major reason for the pattern of the dynamic ^{31}P NMR spectra (i.e., cleavage of the dinuclear dications and appearance of signals corresponding to the mononuclear anions). Interestingly, the formation of the Ag_2S_2 core resulted in a short transannular Ag(1)···Ag(2) distance [3.0287(6) Å] which might suggest an intermetallic interaction [c.f. $\sum r_{\mathrm{vdW}}$(Ag,Ag) = 3.4 Å].[19] In the mononuclear unit, the P−Ag−S fragment is close to the linearity [P(2)−Ag(1)−S(2), 151.77(6)°; P(1)−Ag(2)−S(1), 149.09(6)°]. If the additional Ag−S interactions leading to the dimer unit is considered, the coordination geometry around Ag(I) atoms is best described as distorted T-shaped (or, alternatively, as distorted trigonal planar). Consequently, this arrangement in the Ag_2S_2 core can be considered as a consequence of steric repulsions between the two monomers. The dinuclear

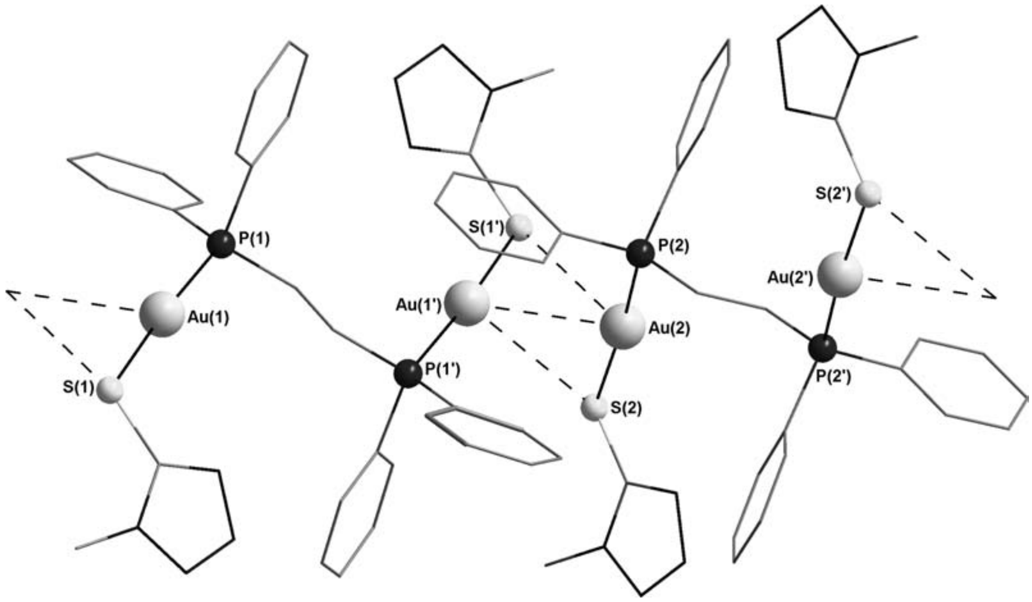

Figure 5. Chain polymer association of alternating **4a** and **4b** molecules in the crystal of **4**, based on Au···Au and S···Au interactions. Hydrogen atoms are removed for clarity; symmetry equivalent atoms are $(1-x, -y, 1-z)$ and $(1-x, 1-y, -z)$, denoted by the "prime" (′) and "double prime" (″) symbols, respectively. Selected bond distances (Å): Au(1′)···Au(2), 3.1038(4); S(1′)···Au(2), 3.3821(19); S(2)···Au(1′), 3.4370(16).

dication of **5** also exhibits weak intramolecular (C)H···Ag agostic interactions, similar to those we found in gold(I) complexes **3** and **4** (i.e., H(26)···Ag(1), 2.95 Å; H(12)···Ag(2), 3.05 Å [c.f. $\sum r_{vdW}$(Ag,H) = 3.15 Å].[19] In the crystal of **5**, the triflate counterions are involved in weak Ag···O cation−anion interactions [2.998(5) and 3.067(5) Å, c.f. $\sum r_{vdW}$(Ag,O) = 3.1 Å].[19]

Selected data and parameters from the X-ray data collection and structure refinement are given in Table 1.

Theoretical Calculations. For a better understanding of the bonding between the phosphine ligands and the gold-containing fragments, theoretical calculations at the density functional theory (DFT) level were carried out on models of compounds **1**−**5**. To reduce the computation time, the phenyl groups were replaced by methyl groups in the phosphine ligands. Details regarding computational procedures can be found in the Experimental Section. Comparisons of salient experimental bond lengths and bonding angles of the measured molecular structures to the theoretically calculated structures are listed in Tables S7−S12 in the Supporting Information.

For model system **2A**, the largest differences between the calculated arrangement and the measured structure was found for the S−Au−P angle (5.2%). This small difference for the bonding angle is not surprising, taking into account that [Au(SCN_4Me)(PPh_3)] (**2**) forms dimers in the solid state through Au···S interactions.[9b] The S−Au and P−Au bond lengths are 0.02 Å larger in the theoretical model than the experimentally determined values found for **2**. The N···Au distance is 0.08 Å larger in **2A** than in **2**.[9b] To estimate the stabilization energy of the Au···N interaction, an investigation of the energy barrier for the rotation of the tetrazole fragment around the S−C bond was carried out. The energy minimum corresponds to a N(Me)−C−S−Au torsion angle of 178.56°, a value which is 6.42% larger than that observed (167.79°) in the solid state. The calculated energy required for the rotation of the tetrazole fragment around the S−C bond is 5.77 kcal/mol. This value indicates that the rotation is possible at room temperature.

In the theoretical model **3A**, the largest differences were found for the Au···Au interactions, which are overestimated by 7.6% and 11.4%, with respect to molecules **3a** and **3b**, respectively. The calculated Au−P and Au−S bond lengths are slightly longer (0.01−0.03 Å) than those found in the molecular structure determined by XRD on single crystals. The calculated P−C−P angle was determined to be 0.25° smaller and 1.75° larger than those measured for molecules **3a** and **3b**, respectively. The calculated P−Au−S angles display relative deviations ranging from −1.0% to 5.5% and the Au−S−C angles show relative deviations ranging from 1.7% to 4.9%. Important differences between model **3A** and [{Au(SCN_4Me)}$_2$(μ-dppm)] (**3**) are found in the orientation of the tetrazole rings. Thus, in **3A**, the Au···Au−S−C angles are −72.21° and 67.63°, whereas they are 80.13° and −135.17° in molecule **3a**, and −72.36° and 161.61° in the molecule **3b**, respectively. These values suggest that intermolecular interactions between the tetrazole groups and the hydrogen atoms play an important role for the geometry that the molecules adopt in the solid state. In contrast to the solid-state structure of **3**, in the calculated model system **3A**, there are short intramolecular N···H contacts between the hydrogen atoms of the methyl group of a SCN_4Me unit and the nitrogen atoms of the tetrazole-5-thiolate unit bonded to the other gold atom of the molecule (see Table S8 in the Supporting Information).

To investigate if model **3A** has geometry similar to that found in the measured structure **3** when the correlation effects are included, a geometry optimization at the MP2 level was carried out.[26] The Au···Au distance is 3.15342 Å, which is 0.304 Å shorter than the value calculated at the BP86/TZ2P level. The P−Au bond lengths have relative deviations ranging from 0.7% to 1.0%, whereas the Au−S and S−C bond lengths have relative deviations between 5.9% and 6.0%, compared to the values found for **3**. The P−Au−S and Au−S−C bonding angles are smaller than those found in the crystal structure. Also, in the optimized arrangement of model **3A** at the MP2 level, a short intramolecular N···H contact of 2.59 Å is present.

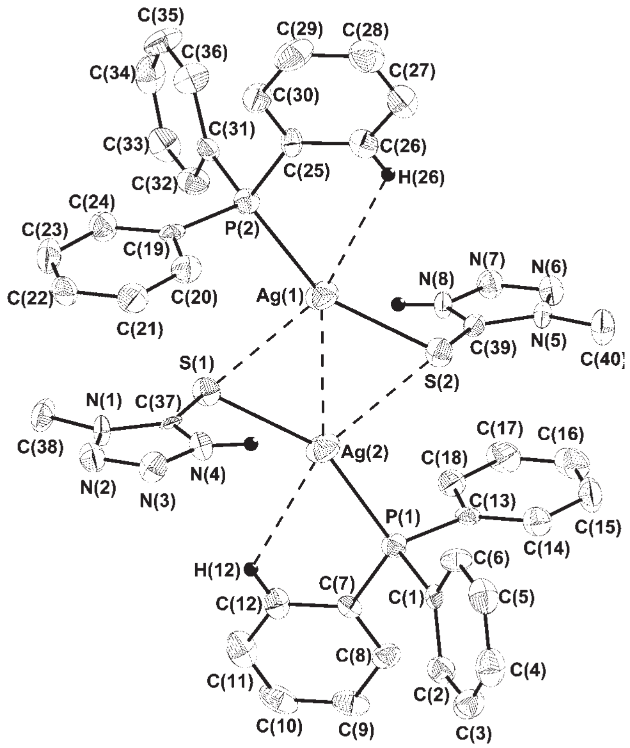

Figure 6. Structure of the dinuclear dication in **5**, showing the atom numbering scheme. Displacement ellipsoids are depicted at the 50% probability level. Hydrogen atoms (except those involved in agostic interactions and those bonded to tetrazole) are omitted for the sake of clarity. Selected bonds lengths (Å): Ag(1)···Ag(2), 3.0287(6); Ag(1)−S(1), 2.9434(15); Ag(1)−S(2), 2.4802(17); Ag(1)−P(2), 2.4047(17); Ag(2)−S(1), 2.4632(16); Ag(2)−S(2), 2.9305(15); Ag(2)−P(1), 2.3980(16); C(12)···Ag(2), 3.647(6); H(12)···Ag(2), 3.05; C(26)···Ag(1), 3.568(6); H(26)···Ag(1), 2.95; angles (°): S(1)−Ag(1)−S(2), 112.03(5); S(1)−Ag(2)−S(2), 112.98(5); Ag(1)−S(1)−Ag(2), 67.46(4); Ag(1)−S(2)−Ag(2), 67.49(4); P(1)−Ag(2)−S(1), 149.09(6); P(2)−Ag(1)−S(2), 151.77(6); P(2)−Ag(1)−S(1), 95.59(5); P(1)−Ag(2)−S(2), 97.10(5); C(12)−H(12)···Ag(2), 122.1(3); C(26)−H(26)···Ag(1), 123.5(3).

The bond lengths and the bonding angles in model system **4A** calculated at DFT are slightly overestimated. The largest deviation, compared to the structure of **4** (5.0%), was found for the Au−S−C bonding angle.

Calculations on the dication dimer $[Ag(HSCN_4Me)(PMe_3)]_2^{2+}$ (**5B**) did not reproduce the geometry found for the $[Ag(HSCN_4Me)(PPh_3)]_2^{2+}$ cation in the solid state. The Ag···Ag distance is 5.1754 Å, 70.9% larger than the distance determined for **5**. Also, in the model system $[Ag(HSCN_4Me)(PMe_3)]_2(OTf)_2$ (**5C**), optimized at the BP86/TZ2P theory level, the equilibrium geometry is not consistent with the arrangement found in **5**. Although the covalent and coordinative bonds compare well to the experimental values, the secondary bonding Ag···Ag and Ag···S distances are 30.0%−36.6% larger in **5C** than the corresponding values of **5**. The calculated Ag···O distances are shorter or larger than the experimental ones (see Table S12 in the Supporting Information). Nevertheless, the arrangement found in **5C** is closer to the geometry found in **5**, compared to that found in the dication **5B**, thus suggesting that the secondary interactions between the anions and the dication play an important role for the stability of the Ag_2S_2 core.

The energy decomposition analysis (EDA) method was employed before to describe the coordinative bonds of phosphine ligands to transition-metal centers.[27,28] A detailed description of the terms used in the analysis of the bonding energy can be found elsewhere.[28] A summary of the EDA of P−M bonds for models **2A** and the mononuclear cation $[Ag(HSCN_4Me)(PMe_3)]^+$ (**5A**) is listed in Table 2.

The bond dissociation energy, ΔE (where $\Delta E = -De$), of the phosphine ligands is 6 kcal/mol smaller for **5A**, compared to **2A**. The ionic (**2A**, 72.32%; **5A**, 71.22%) and covalent (**2A**, 27.68%; **5A**, 28.78%) contributions to the bonding energy have comparable values. These results are similar to those reported for the complexes of $[(Me_3P)M(CO)_5]$ (M = Cr, Mo, W), where the percentage of the electrostatic interaction also is greater than that of the covalent contributions.

In summary, the theoretical calculations at the BP86/TZ2P level on models of the complexes **2** and **4** are consistent with the geometries found via XRD on single crystals. The bonding between the gold-tetrazole-5-thiolato fragments and methylphosphine ligands is mainly electrostatic. The bonding in the monomeric cation **5A** is slightly weaker than that found in the gold neutral analogue, **2A**. The Au···Au interactions found in **3** are better described by calculations at the MP2 level of theory.

■ CONCLUSIONS

In conclusion, we have developed an efficient method to prepare metal−thiotetrazole complexes. The molecular structures established by single-crystal XRD confirm their initial formulation suggested by IR and NMR analyses. However, a different structural framework was observed for **5**, which crystal contains a dinuclear dication built through bridges established by sulfur atoms of the thione tautomers of **1**. Intramolecular Au···Au interactions were detected in **3**, whereas in **4**, intermolecular aurophilic bonding leads to the formation of a chain polymer. As indicated by IR and confirmed by single-crystal XRD in gold(I) tetrazole-5-thiolates **2**, **3**, and **4**, the coordination also occurs through the nitrogen atom. The weak agostic interactions (C)H···M observed in the measured structures are consistent with those mentioned in the literature. Nevertheless, they provide additional stability for the structures.

■ EXPERIMENTAL SECTION

General. All manipulations were carried out under vacuum or argon, using standard Schlenk line techniques in anhydrous solvents. Dry tetrahydrofuran (THF) was obtained by distillation under argon over sodium and benzophenone. All other solvents and reagents were purchased from commercial suppliers and used without further purification. Other starting materials were prepared according to the literature: $[AuCl(PPh_3)]$,[29] $[Au_2Cl_2(\mu\text{-dppm})]$,[30] $[Au_2Cl_2(\mu\text{-dppe})]$,[31] $[Ag(OTf)(PPh_3)]$.[32] ^1H, ^{13}C, ^{19}F, and ^{31}P NMR were recorded using various spectrometers (Jeol Eclipse 270, Jeol Eclipse 400, Bruker DPX-500, and Bruker-360). The spectra were measured in $CDCl_3$ or CD_2Cl_2. The chemical shifts (δ) are quoted in units of ppm, relative to external standards Me_4Si (^1H, ^{13}C), 85% H_3PO_4 (^{31}P), and CCl_3F (^{19}F). Multiplicities are abbreviated as follows: br, broad; s, singlet; d, doublet; t, triplet; and m, multiplet. Coupling constants (J) are given in Hertz (Hz). The mass spectra were obtained via an electrospray ionization (ES) technique, using a Finnigan LCQ instrument. Melting points were determined using differential scanning calorimetry (Linseis DSC PT-10 instrument). Measurements were performed at a heating rate of 5 °C/min in closed aluminum containers with a hole (1 μm) on the top for gas

Table 1. Crystallographic Data for 3−5

	3	4	5
formula	$C_{29}H_{28}Au_2N_8P_2S_2$	$C_{30}H_{30}Au_2N_8P_2S_2$	$C_{42}H_{38}Ag_2N_8P_2S_4F_6O_6$
FW [g/mol]	1008.61	1022.64	1270.76
crystal system	triclinic	triclinic	monoclinic
space group	$P\bar{1}$(2)	$P\bar{1}$(2)	$P21/c$ (14)
color/habit	colorless plate	colorless block	colorless plate
size [mm^3]	0.15 × 0.13 × 0.03	0.2 × 0.2 × 0.1	0.3 × 0.1 × 0.02
a [Å]	12.6579(3)	13.2564(7)	20.7270(12)
b [Å]	15.1948(3)	13.5584(7)	9.0502(4)
c [Å]	17.7332(4)	15.7146(9)	28.0743(15)
α [deg]	89.517(2)	68.583(5)	90
β [deg]	74.754(2)	72.896(5)	109.715(6)
γ [deg]	78.006(2)	69.334(5)	90
V [Å^3]	3214.97(13)	2415.6(2)	4957.6(5)
Z	4	3	4
ρ_{calcd}[g/cm^3]	2.084	2.109	1.703
μ[mm^{-1}]	9.380	9.365	1.100
F(000)	1912	1458	2544
$\lambda_{Mo\ K\alpha}$[Å]	0.71073	0.71073	0.71073
T [K]	100	173	200
θ min/max [°]	4.11/26.00	4.09/26.00	4.18/25.09
Refl. collected	49623	17509	18778
Refl. Independ.	12595	9462	8705
Refl. observed	8836	6542	3054
No. parameters	775	597	639
R_{int}	0.0578	0.0455	0.0810
R_1 (obs)	0.0436	0.0556	0.1511
wR_2 (all data)	0.0428	0.0537	0.0445
S	0.785	0.850	0.568
resd. dens. [e/Å^3]	−0.80, 1.46	−1.80, 1.60	−0.62, 0.56
device type	Oxford Xcalibur3 CCD	Oxford Xcalibur3 CCD	Oxford Xcalibur3 CCD
solution	SIR-92	SIR-92	SIR-92
refinement	SHELXL-97	SHELXL-97	SHELXL-97
absorption correction	multiscan	multiscan	multiscan
CCDC	797943	797942	797941

Table 2. Energy Decomposition Analysis of the P−M Bonds in the Model Complexes [Au(SCN$_4$Me)(PMe$_3$)] (2A) and [Ag(HSCN$_4$Me)(PMe$_3$)]$^+$ (5A) at the BP86/TZ2P Level

	Energy (kcal/mol)	
	2A	5A
ΔE_{int}	−61.71	−56.22
ΔE_{Pauli}	182.89	93.48
ΔE_{elstat}	−176.90 (72.32%)[a]	−106.62 (71.22%)[a]
ΔE_{steric}	5.99	−13.14
ΔE_{orb}	−67.71 (27.68%)[a]	−43.08 (28.78%)[a]
ΔE_{prep}	3.23	3.71
ΔE (= −De)	−58.48	−52.51

[a] Values given in parentheses represent the proportion of the sum $E_{elstat}+E_{orb}$.

release with a nitrogen flow of 5 mL/min. IR spectra were measured in the attenuated total reflection mode (ATR) on a Perkin−Elmer Spectrum BX II. Raman spectra were recorded using a Bruker MULTIRAM 1064 2000R NIR FT-Raman instrument equipped with a Nd:YAG laser (1064 nm). The intensities are reported in percentages relative to the most intense peak and are given in parentheses. Thin-layer chromatography (TLC) was performed on aluminum oxide 60 F254 neutral plates or silica-gel-coated aluminum F254 plates from Merck. All plates were visualized by UV irradiation at 254 nm and/or staining with potassium permanganate.

Computational Details. Theoretical calculations at the DFT level were carried out using the ADF software package[33] on models of compounds **2**−**5**, using methylphosphine ligands. The geometries optimizations were performed using the BP86 functional and the TZ2P basis set, as implemented in the ADF software package. The inner electrons were treated by frozen-core approximation, using the large core option. The relativistic effects were considered using the zero-order regular approximation (ZORA). To reduce the calculation time, the model arrangements **4A**, **5B**, and **5C** were optimized in the C_i point group. The energy minima of the equilibrium geometries were verified by frequency calculations. For the arrangements **2A**−**5A**, **5B** and **5C** negative frequencies (1 for **2A** and **5A**, 2 for **3A** and **4A**, 4 for **5B** and **5C**) were obtained in the range of 0−50 cm^{-1}. Calculations of the gradients along the corresponding normal modes for the imaginary frequencies confirmed that the optimized arrangements are energy minima. The bonding between the phosphine ligands and metal centers were investigated using the energy decomposition scheme implemented in ADF,[34] based on the method of Morokuma and Ziegler.[35,36] Model **3A** was studied at the MP2 theory level with a LANL2DZ basis set,[37] using the GAMESS software package.[38] The basis set used for the P atoms was augmented with one polarization and one diffuse function.[39] The data were taken from the EMSL Basis Sets Library.[40] The coordinates of the optimized structures and other relevant data are provided as Supporting Information.

Crystal Structure Analysis. The crystallographic data were collected using an Oxford Xcalibur3 diffractometer with a Spellman generator (voltage of 50 kV, current of 40 mA) and a Kappa CCD area detector with graphite-monochromated Mo Kα radiation (λ = 0.71073 Å). The data collection was undertaken using the CrysAlis CCD software,[41] and the data reduction was performed with the CrysAlis Red software.[42] The structures were solved with SIR-92[43] and refined with SHELXL-97[44] implemented in the program package WinGX[45] and finally checked using PLATON.[46] CCDC file numbers CCDC-797943 (for **3**), CCDC-797942 (for **4**) and CCDC-797941 (for **5**) contain the supplementary crystallographic data for this paper. These data can be obtained free of charge from the Cambridge Crystallographic Data Centre (www.ccdc.cam.ac.uk/data request/cif).

Synthesis of [$HSCN_4Me$] (1). To a solution of MeNCS (50 g, 0.68 mol) in H_2O (500 mL) was added NaN_3 (67.36 g, 1.04 mol). The reaction mixture was stirred under reflux conditions for 6 h. The solution was then cooled and filtered from any insoluble material present. It was extracted twice with Et_2O, to remove any unreacted isothiocyanate. The aqueous layer was cooled and acidified with concentrated HCl (60 mL) to pH 3. Furthermore, it was extracted three times with Et_2O. The organic layer was dried over $MgSO_4$. Afterward, the solvent was evaporated in vacuum. Recrystallization from chloroform and petroleum ether afforded white crystals of **1**. Yield (21.8 g, 28%); m.p. = 124.6−125.9 °C; ^{1}H NMR (400 MHz, $CDCl_3$, 25 °C, TMS) δ = 3.92 (s, 3H, Me), 14.48 ppm (s, H, NH); ^{13}C NMR (100 MHz, $CDCl_3$, 25 °C, TMS) δ = 33.98 (s, Me), 164.02 ppm (s, CN_4-ring); MS (ES$^+$): m/z = 117 $[M+H]^+$.

Synthesis of [Au(SCN_4Me)(PPh_3)] (2). To a solution of $HSCN_4Me$ (0.0096 g, 0.082 mmol) in 15 mL of anhydrous THF was added [AuCl(PPh_3)] (0.041 g, 0.082 mmol), and the reaction mixture was stirred for 3 h at room temperature under argon. The resulting colorless solution was treated dropwise with anhydrous NEt_3 (0.083 g, 0.082 mmol). After stirring for an additional 1 h, the solution was concentrated under reduced pressure and precipitated with hexane to give **2** as a white solid. Yield: 0.038 g (80%); R_f = 0.82 (AcOEt/pentane 3:1); m.p. = 154 °C; ^{1}H NMR (270 MHz, $CDCl_3$, 25 °C, TMS): δ = 3.94 (s, 3H, Me), 7.64−7.53 (m, 9H, H-*ortho*, H-*para*), 7.51−7.44 ppm (m, 6H, H-*meta*); ^{13}C NMR (62 MHz, $CDCl_3$, 25 °C, TMS): δ = 33.9 (s, Me), 128.8 (d, ^1J(C,P) = 40.6 Hz, C-*ipso*), 129.2 (d, ^3J(C,P) = 8.1 Hz, C-*meta*), 131.8 (s, C-*para*), 134.2 (d, ^2J(C,P) = 9.3 Hz, C-*ortho*), 158.1 ppm (s, CN_4-ring); ^{31}P NMR (109 MHz, $CDCl_3$, 25 °C, H_3PO_4 85%) δ = 37.9 ppm (s, P, PPh_3); IR (ATR, cm^{-1}): ν = 967 (vw), 998 (w), 1026 (w), 1037 (w), 1076 (w), 1102 (m) (CN_4 ring), 1269 (w), 1308 (vw) (N−N═N), 692 (vs), 711 (m) (C−S); Raman (100 mW, 25 °C, cm^{-1}): ν = 999 (w), 1027 (m), 1077 (w), 1102 (m) (CN_4 ring), 1270 (m) (−N−N═N), 694 (w), 713 (vw) (C−S), 346 (vw) (Au−S); MS (ES$^+$): m/z = 575.3 $[M+H]^+$, 721.4 $[Au(PPh_3)_2]^+$.

Synthesis of [{Au(SCN_4Me)}$_2$(μ-dppm)] (3). To a solution of $HSCN_4Me$ (0.010 g, 0.086 mmol) in 15 mL of anhydrous THF was added [Au_2Cl_2(μ-dppm)] (0.036 g, 0.043 mmol), and the reaction mixture was stirred for 3 h at room temperature under argon. The resulting yellow solution was treated dropwise with anhydrous NEt_3 (0.087 g, 0.086 mmol). After stirring for an additional 1 h, the solution was concentrated under reduced pressure and precipitated with hexane to give **3** as a light orange solid. Yield: 0.040 g (91%); R_f = 0.48 (AcOEt/pentane 3:1); ^{1}H NMR (500 MHz, $CDCl_3$, 25 °C, TMS): δ = 3.72 (t, ^2J(H,P) = 11.5 Hz, 2H, $-CH_2-$), 3.9 (s, 6H, Me), 7.30 (t, ^3J(H,H) = 7.5 Hz, 8H, H-*meta*), 7.37 (t, ^3J(H,H) = 7.5 Hz, 4H, H-*para*), 7.7 ppm (dd, ^3J(H,H) = 7 Hz, ^3J(H,P) = 21 Hz 8H, H-*ortho*); ^{13}C NMR (100 MHz, $CDCl_3$, 25 °C, TMS): δ = 29.6 (s, $-CH_2-$), 34.1 (s, Me), 128.1 (t, ^1J(C, P) = 31 Hz, C-*ipso*), 129.4 (t, ^3J(C,P) = 6.5 Hz, C-*meta*), 132.2 (s, C-*para*), 133.5 (t, ^2J(C,P) = 8 Hz, C-*ortho*), 158.3 ppm (s, CN_4-ring); ^{31}P NMR (162 MHz, $CDCl_3$, 25 °C, H_3PO_4 85%): δ = 30.9 ppm (s, 2P, PPh_2); IR (ATR, cm^{-1}): ν = 970 (w), 998 (w), 1027 (w), 1100 (s) (CN_4 ring), 1269 (m), 1316 (vw) (N−N═N), 704 (vw), 688 (vs) (C−S); Raman (100 mW, 25 °C, cm^{-1}): ν = 999 (vs), 1028 (m), 1082 (w), 1103 (w) (CN_4 ring), 1271 (m) (−N−N═N), 683 (w), 706 (w) (C−S), 343 (vw) (Au−S); MS (ES$^+$): m/z = 893.1 $[Au_2(SCN_4Me)(\mu\text{-dppm})]^+$.

Synthesis of [{Au(SCN_4Me)}$_2$(μ-dppe)] (4). To a solution of $HSCN_4Me$ (0.010 g, 0.086 mmol) in 15 mL of anhydrous THF was added [Au_2Cl_2(μ-dppe)] (0.037 g, 0.043 mmol), and the reaction mixture was stirred for 3 h at room temperature under argon. The resulting yellow solution was treated dropwise with anhydrous NEt_3 (0.087 g, 0.086 mmol). After stirring for an additional 1 h, the solution was concentrated under reduced pressure and precipitated with hexane to give **4** as a yellow solid. Yield: 0.035 g (81%); R_f = 0.77 (AcOEt/pentane 3:1); ^{1}H NMR (500 MHz, $CDCl_3$, 25 °C, TMS): δ = 3.07 (s, br, 4H, $-CH_2-CH_2-$), 3.9 (s, 6H, Me), 7.5−7.47 (m, 12H, H-*meta* + H-*para*), 7.98−7.95 ppm (m, 8H, H-*ortho*); ^{31}P NMR (109 MHz, $CDCl_3$, 25 °C, H_3PO_4 85%): δ = 38.2 ppm (s, 2P, PPh_2); IR (ATR, cm^{-1}): ν = 967 (w), 997 (w), 1026 (w), 1037 (w), 1077 (w), 1106 (w) (CN_4 ring), 1264 (w), 1276 (m), 1318(w) (−N−N═N), 690 (s), 702 (s), 698 (s) (C−S); Raman (100 mW, 25 °C, cm^{-1}): ν = 1000 (vs), 1028 (m), 1078 (vw), 1107 (w) (CN_4 ring), 1277 (m) (−N−N═N), 699(w), 706 (m) (C−S), 339 (s) (Au−S), MS (ES$^+$): m/z = 907.1 $[Au_2(SCN_4Me)(\mu\text{-dppe})]^+$, 824.1 $[Au_2S(\mu\text{-dppe})]^+$.

Synthesis of [Ag($HSCN_4Me$)(PPh_3)]$_2$(OTf)$_2$ (5). To a solution of $HSCN_4Me$ (0.021 g, 0.188 mmol) in 20 mL of anhydrous CH_2Cl_2 was added [Ag(OTf)(PPh_3)] (0.097 g, 0.187 mmol), and the reaction mixture was stirred for 2 h without light, at room temperature under argon. The resulting colorless solution was concentrated under reduced pressure and precipitated with hexane to give **5** as a white solid. Yield: 0.041 g (85%); R_f = 0.91 (AcOEt/pentane 3:1); m.p. = 159 °C; ^{1}H NMR (500 MHz, $CDCl_3$, 25 °C, TMS): δ = 3.8 (s, 6H, Me), 7.4−7.39 ppm (m, 15H, H-*ortho* + H-*meta* + H-*para*); ^{13}C NMR (90 MHz, $CDCl_3$, 25 °C, TMS): δ = 34.5 (s, Me), 120.06 (d, ^1J(C,P) = 319.4 Hz, C-*ipso*); 129.09 (s, C-*meta*), 130.8 (s, C-*para*), 133.7 (d, ^2J(C,P) = 15.3 Hz, C-*ortho*), 161.4 ppm (s, CN_4-ring); ^{31}P NMR (162 MHz, CD_2Cl_2, 25 °C, H_3PO_4 85%): δ = 11.4 ppm (s, 2P, PPh_3); ^{31}P NMR (162 MHz, CD_2Cl_2, −85 °C, H_3PO_4 85%): δ = 10.3 (dd, ^1J(P,^{107}Ag) = 417.5, ^1J(P,^{109}Ag) = 481.0 Hz), 11.3 (dd, ^1J(P,^{107}Ag) = 318.5, ^1J(P,^{109}Ag) = 367.6 Hz); IR (ATR, cm^{-1}): ν = 960 (w), 1014 (vs), 1072 (w), 1097 (m) (CN_4 ring), 1524 (m) (N−C═S), 1337 (m), 1014 (ws), 750 (s) (C═S), 1233 (s) ($\nu_{as}SO_3$), 1203 (vs) (ν_s CF_3), 1164 (s) ($\nu_{as}CF_3$), 1042 (w) (ν_sSO_3); Raman (100 mW, 25 °C, cm^{-1}): ν = 999 (vs), 1026 (m) (CN_4 ring), 1285 (vw) (N−N═N), 1586 (m) (N−C═S), 2966 (w), 3060 (m), 3142 (vw), 3169 (vw) (N−H and C−H), 758 (w), 1343 (m) (C═S), 1234 (vw) ($\nu_{as}SO_3$), 1183 (vw) (ν_sCF_3), 1157 (vw) ($\nu_{as}CF_3$), 1097 (w) (ν_sSO_3), 350 (vw) (Ag−S); MS (ES$^+$): m/z = 631.2 $[Ag(PPh_3)_2]^+$.

■ ASSOCIATED CONTENT

S Supporting Information. NMR spectra, XRD studies, and theoretical calculations. The crystal structures of compounds **3**, **4**, and **5** have been deposited at the Cambridge Crystallographic Data Centre and allocated the deposition numbers CCDC-797943, CCDC-797942, and CCDC-797941. This material is available free of charge via the Internet at http://pubs.acs.org.

■ AUTHOR INFORMATION

Corresponding Author

* Fax: (+49)89-2180-77398. E-mail: konstantin.karaghiosoff@cup.uni-muenchen.de.

■ ACKNOWLEDGMENT

Financial support from Deutscher Akademischer Austausch Dienst (DAAD), CNCSIS-UEFISCSU TD66/2007 (Romania) is gratefully acknowledged.

■ REFERENCES

(1) (a) Sutton, B. M.; McGusty, E.; Walz, D. T.; DiMartino, M. J. *J. Med. Chem.* **1972**, *15*, 1095–1098. (b) Lorber, A.; Simon, T. M. *Gold Bull.* **1979**, *12*, 149–158. (c) Shaw, C. F., III; Beery, A.; Stocco, G. C. *Inorg. Chim. Acta* **1986**, *123*, 213–216.

(2) Bain, C. D.; Whitesides, G. M. *Angew. Chem., Int. Ed.* **1989**, *28*, 506–512.

(3) (a) Dash, K. C.; Schmidbaur, H. *Met. Ions Biol. Syst.* **1982**, *14*, 179–205. (b) *Gold Progress in Chemistry, Biochemistry and Technology*; Schmidbaur, H., Ed.; Wiley: Chichester, U.K., 1999.

(4) (a) Lee, K.; Kim, Y.-J.; Baeck, K. K. *J. Organomet. Chem.* **2005**, *690*, 4319–4329. (b) Ng, V. W. L.; Kuan, S.-L.; Leong, W. K.; Koh, L. L.; Tan, G. K.; Goh, L. Y.; Webster, R. D. *Inorg. Chem.* **2005**, *44*, 5229–5240. (c) Ma, C.; Sun, J. *Polyhedron* **2004**, *23*, 1547–1555.

(5) (a) Butler, R. N. In *Comprehensive Heterocyclic Chemistry II*, Vol. 4; Katritzky, A. R., Rees, C. W., Scriven, E. F. V., Eds.; Pergamon: New York, 1996; pp 621−678. (b) Ostrovskii, V. A.; Koldobskii, G. I.; Trifonov, R. E. In *Comprehensive Heterocyclic Chemistry III*, Vol. 6; Katritzky, A. R., Ramsden, C. A., Scriven, E. F. V., Taylor, R. J. K., Zhdankin, V. V., Eds.; Elsevier: Oxford, Tokyo, 2008, pp 257−423.

(6) (a) Naoto, O.; Hideki, M. Jpn. Patent JP 2002107865 A, 2002. [*Chem. Abstr.* **2002**, *136*, 301718.] (b) Lam, W. K.; Lok, R.; Sandford, D. W. U.S. Patent 6,322,961 B1, 2001. [*Chem. Abstr.* **2001**, *136*, 12757.] (c) Ichikawa, S.; Inaba, T.; Yoshikawa, S. Jpn. Patent JP 2001281784 A, 2001. [*Chem. Abstr.* **2001**, *135*, 296125.] (d) Yoshikawa, S.; Mifune, H. Jpn. Patent JP 2001281783 A, 2001. [*Chem. Abstr.* **2001**, *135*, 296124.] (e) Sasaki, H.; Yoshikawa, S. Jpn. Patent JP 2001100352 A, 2001. [*Chem. Abstr.* **2001**, *134*, 287806.] (f) Yoshikawa, S.; Sasaki, H. Jpn. Patent JP 2001075216 A, 2001. [*Chem. Abstr.* **2001**, *134*, 259139.] (g) Yoshikawa, S.; Sasaki, H.; Matsunaga, A. Jpn. Patent JP 2001075214 A, 2001. [*Chem. Abstr.* **2001**, *134*, 259138.] (h) Brant, S. E.; Cleary, B. P.; Lok, R.; White, W. W. Jpn. Patent JP 2000147703 A, 2000. [*Chem. Abstr.* **2000**, *133*, 10957.] (i) Lok, R.; White, W. W.; Marshall, M. W. U.S. Patent 5,912,112 A, 1999. [*Chem. Abstr.* **2000**, *131*, 25698.]

(7) Nichick, M. N.; Voitekhovich, S. V.; Shavel, A.; Lesnikovich, A. I.; Ivashkevich, O. A. *Polyhedron* **2009**, *28*, 3138–3142.

(8) (a) Agarwala, U.; Singh, B. *Indian J. Chem.* **1969**, *7*, 726–728. (b) Johar, G. S.; Agarwala, U. *J. Indian Chem. Soc.* **1970**, *47*, 904–906.

(9) (a) Beck, W.; Burger, K.; Keubler, M. *Z. Anorg. Allg. Chem.* **1977**, *428*, 173–186. (b) Noth, H.; Beck, W.; Burger, K. *Eur. J. Inorg. Chem.* **1998**, 93–99.

(10) (a) Schmidbaur, H. *Gold Bull.* **1990**, *23*, 11–21. (b) Schmidbaur, H. *Gold Bull.* **2000**, *33*, 3–10. (c) Schmidbaur, H. *Chem. Soc. Rev.* **1995**, *24*, 391–400. (d) Schmidbaur, H.; Schier, A. *Chem. Soc. Rev.* **2008**, *37*, 1931–1951. (e) Pyykko, P. *Chem. Rev.* **1997**, *97*, 597–636. (f) Pyykko, P. *Chem. Soc. Rev.* **2008**, *37*, 1967–1997.

(11) (a) Abram, U.; Mack, J.; Ortner, K.; Muller, M. *J. Chem. Soc., Dalton Trans.* **1998**, 1011–1019. (b) Lang, E. S.; Dahmer, M.; Abram, U. *Acta Crystallogr., Sect. C: Cryst. Struct. Commun.* **1999**, *C55*, 854–856. (c) Ortner, K.; Abram, U. *Polyhedron* **1999**, *18*, 749–754.

(12) Cea-Olivares, R.; Jimenez-Sandoval, O.; Hernandez-Ortega, S.; Sanchez, M.; Toscano, R. A.; Haiduc, I. *Heteroat. Chem.* **1995**, *6*, 89–97.

(13) Lieber, E.; Ramachandran, J. *Can. J. Chem.* **1959**, *37*, 101–109.

(14) (a) Muetterties, E. L.; Alegranti, C. W. *J. Am. Chem. Soc.* **1972**, *94*, 6386–6391. (b) Barron, P. F.; Dyason, J. C.; Healy, P. C.; Engelhardt, L. M.; Skelton, B. W.; White, A. H. *J. Chem. Soc., Dalton Trans.* **1986**, 1965–1970. (c) Caballero, A.; Guerrero, A.; Jalon, F. A.; Manzano, B. R.; Claramunt, R. M.; Santa Maria, M. D.; Escolastico, C.; Elguero, J. *Inorg. Chim. Acta* **2003**, *347*, 168–174.

(15) (a) Socol, S. M.; Verkade, J. G. *Inorg. Chem.* **1984**, *23*, 3487–3493. (b) Bachman, R. E.; Andretta, D. F. *Inorg. Chem.* **1998**, *37*, 5657–5663. (c) Cingolani, A.; Efendi; Marchetti, F.; Pettinari, C.; Pettinari, R.; Skelton, B. W.; White, A. H. *Inorg. Chim. Acta* **2002**, *329*, 100–112. (d) Sekabunga, E. J.; Smith, M. L.; Webb, T. R.; Hill, W. E. *Inorg. Chem.* **2002**, *41*, 1205–1214. (e) Verkade, J. G.; Mosbo, J. A. In *Phosphorus-31 NMR Spectroscopy in Stereochemical Analysis*; Verkade, J. G., Quin, L. D., Eds.; VCH: Weinheim, Germany, 1987.

(16) Barrow, M.; Burgi, H.-B.; Camalli, M.; Caruso, F.; Fischer, E.; Venanzi, L. M.; Zambonelli, L. *Inorg. Chem.* **1983**, *22*, 2356–2362.

(17) Szafranski, C. A.; Tanner, W.; Laibinis, P. E.; Garrell, R. L. *Langmuir* **1998**, *14*, 3570–3579.

(18) Nakamoto, K. *Infrared and Raman Spectra of Inorganic and Coordination Compounds*, 6th ed.; Wiley: Hoboken, NJ, 2009; pp 103.

(19) (a) *Die Elemente*; Walter de Gruyter: Berlin, 1994. (b) Huheey, J. E. *Inorganic Chemistry*, 3rd ed.; Harper Collins: New York, 1983.

(20) (a) Basch, H.; Ratner, M. A. *J. Chem. Phys.* **2004**, *120*, 5771–5780. (b) Calhorda, M. J. *Chem. Commun.* **2000**, 801–809. (c) Friedrichs, S.; Jones, P. G. *Z. Naturforsch.* **2004**, *59b*, 49–57. (d) Friedrichs, S.; Jones, P. G. *Z. Naturforsch.* **2004**, *59b*, 793–801. (e) Friedrichs, S.; Jones, P. G. *Z. Naturforsch.* **2004**, *59b*, 1429–1437. (f) Baukova, T. V.; Kuzmina, L. G.; Oleinikova, N. A.; Lemenovskii, D. A.; Blumenfel'd, A. L. *J. Organomet. Chem.* **1997**, *530*, 27–38. (g) Baukova, T. V.; Kuzmina, L. G.; Oleinikova, N. A.; Lemenovskii, D. A. *Izv. Akad. Nauk, Ser. Khim.* **1995**, 2023–2034. (h) Raisanen, M. T.; Runeberg, N.; Klinga, M.; Nieger, M.; Bolte, M.; Pyykko, P.; Leskela, M.; Repo, T. *Inorg. Chem.* **2007**, *46*, 9954–9960.

(21) (a) Ingleson, M. J.; Mahon, M. F.; Patmore, N. J.; Ruggiero, G. D.; Weller, A. S. *Angew. Chem., Int. Ed.* **2002**, *41*, 3694–3697. (b) Gerasimchuk, N.; Esaulenko, A. N.; Dalley, K. N.; Moore, C. *Dalton Trans.* **2010**, *39*, 749–764. (c) Liu, C.-S.; Chen, P.-Q.; Chang, Z.; Wang, J.-J.; Yan, L.-F.; Sun, H.-W.; Bu, X.-H.; Lin, Z.; Li, Z.-M.; Batten, S. R. *Inorg. Chem. Commun.* **2008**, *11*, 159–163. (d) Clarke, A. J.; Ingleson, M. J.; Kociok-Kohn, G.; Mahon, M. F.; Patmore, N. J.; Rourke, J. P.; Ruggiero, G. D.; Weller, A. S. *J. Am. Chem. Soc.* **2004**, *126*, 1503–1517. (e) Atakol, O.; Fuess, H.; Kurtaran, R.; Akay1, A.; Arici, C.; Ergun, U.; Emregul, K. C. *J. Therm. Anal. Calorim.* **2007**, *90*, 517–523.

(22) (a) Nunokawa, K.; Onaka, S.; Mizuno, Y.; Okazaki, K.; Sunahara, T.; Ito, M.; Yaguchi, M.; Imai, H.; Inoue, K.; Ozeki, T.; Chiba, H.; Yosida, T. *J. Organomet. Chem.* **2005**, *690*, 48–56. (b) Nunokawa, K.; Onaka, S.; Tatematsu, T.; Ito, M.; Sakai, J. *Inorg. Chim. Acta* **2001**, *322*, 56–64. (c) Onaka, S.; Yaguchi, M.; Yamauchi, R.; Ozeki, T.; Ito, M.; Sunahara, T.; Sugiura, Y.; Shiotsuka, M.; Nunokawa, K.; Horibe, M.; Okazaki, K.; Iida, A.; Chiba, H.; Inoue, K.; Imai, H.; Sako, K. *J. Organomet. Chem.* **2005**, *690*, 57–68. (d) Jia, G; Puddephatt, R. J.; Vittal, J. J. *Polyhedron* **1992**, *11*, 2009–2014. (e) Bardaji, M.; Connelly, N. G.; Gimeno, M. C.; Jones, P. G.; Laguna, A.; Laguna, M. *J. Chem. Soc., Dalton Trans.* **1995**, 2245–2250. (f) Uson, R.; Laguna, A.; Laguna, M.; Jimenez, J.; Gomez, M. P.; Sainz, A. *J. Chem. Soc., Dalton Trans.* **1990**, 3457–3463. (g) Colacio, E.; Romerosa, A.; Ruiz, J.; Roman, P.; Gutierrez-Zorilla, J. M.; Vegas, A.; Martinez-Ripoll, M. *Inorg. Chem.* **1991**, *30*, 3743–3749.

(23) (a) Crespo, O.; Gimeno, M. C.; Laguna, A.; Kulcsar, M.; Silvestru, C. *Inorg. Chem.* **2009**, *48*, 4134–4142. (b) Canales, S.; Crespo, O.; Gimeno, M. C.; Jones, P. G.; Laguna, A. *Inorg. Chem.* **2004**, *43*, 7234–7238.

(24) Artigas, M. M.; Crespo, O.; Gimeno, M. C.; Jones, P. G.; Laguna, A.; Villacampa, M. D. *Inorg. Chem.* **1997**, *36*, 6454–6456.

(25) Heinrich, D. D.; Fackler, J. P.; Lahuerta, P. *Inorg. Chim. Acta* **1986**, *116*, 15–19.

(26) (a) Fernandez, E. J.; Concepcion Gimeno, M.; Jones, P. G.; Laguna, A.; Laguna, M.; Lopez-de-Luzuriaga, J. M.; Rodriguez, M. A. *Chem. Ber.* **1995**, *128*, 121–124. (b) Pyykkö, P.; Mendizabal, F. *Inorg.

Chem. **1998**, *37*, 3018–3025. (c) Fernandez, E. J.; Lopez-de-Luzuriaga, J. M.; Monge, M.; Rodriguez, M. A.; Crespo, O.; Concepcion Gimeno, M.; Laguna, A.; Jones, P. G. *Inorg. Chem.* **1998**, *37*, 6002–6006.

(27) Frenking, G.; Wichmann, K.; Frohlich, N.; Grobe, J.; Golla, W.; Van, D. L.; Krebs, B.; Lage, M. *Organometallics* **2002**, *21*, 2921–2930.

(28) Frenking, G.; Wichmann, K.; Froehlich, N.; Loschen, C.; Lein, M.; Frunzke, J.; Rayon, V. M. *Coord. Chem. Rev.* **2003**, *238*−*239*, 55–82.

(29) (a) Al-Saady, A. K.; McAuliffe, C. A.; Parish, R. V.; Sandbank, J. A. *Inorg. Synth.* **1985**, *23*, 191–194. (b) Bruce, M. I.; Nicholson, B. K.; Shawkataly, O. B. *Inorg. Synth.* **1989**, *26*, 324–326.

(30) Schmidbaur, H.; Wohlleben, A.; Wagner, F.; Orama, O.; Huttner, G. *Chem. Ber.* **1977**, *110*, 1748–1754.

(31) Cariati, F.; Naldini, L.; Simonetta, G.; Malatesta, L. *Inorg. Chim. Acta* **1967**, *1*, 315–318.

(32) Lettko, L.; Wood, J. S.; Rausch, M. D. *Inorg. Chim. Acta* **2000**, *308*, 37–44.

(33) (a) te Velde, G.; Bickelhaupt, F. M.; Baerends, E. J.; Guerra, C. F.; van Gisbergen, S. J. A.; Snijders, J. G.; Ziegler, T. *J. Comput. Chem.* **2001**, *22*, 931–967. (b) Fonseca Guerra, C.; Snijders, J. G.; te Velde, G.; Baerends, E. J. *Theor. Chem. Acc.* **1998**, *99*, 391–403. (c) *ADF2008.01e, SCM, Theoretical Chemistry*; Vrije Universiteit: Amsterdam, http://www.scm.com. (For the complete reference, see the Supporting Information.)

(34) Bickelhaupt, F. M.; Baerends, E. J. In *Reviews in Computational Chemistry*, Vol. 15; Lipkowitz, K. B., Boyd, D. B., Eds.; Wiley−VCH: New York, 2000; pp 1−86.

(35) (a) Morokuma, K. *J. Chem. Phys.* **1971**, *55*, 1236–1244. (b) Kitaura, K.; Morokuma, K. *Int. J. Quantum Chem.* **1976**, *10*, 325–340.

(36) Ziegler, T.; Rauk, A. *Theor. Chem. Acc.* **1977**, *46*, 1–10.

(37) (a) Dunning, T. H., Jr.; Hay, P. J. In *Methods of Electronic Structure Theory*, Vol. 2; Schaefer , H. F., III, Ed.; Plenum Press: New York, 1977. (b) Hay, P. J.; Wadt, W. R. *J. Chem. Phys.* **1985**, *82*, 270–283. (c) Wadt, W. R.; Hay, P. J. *J. Chem. Phys.* **1985**, *82*, 284–298. (d) Hay, P. J.; Wadt, W. R. *J. Chem. Phys.* **1985**, *82*, 299–310.

(38) (a) Schmidt, M. W.; Baldridge, K. K.; Boatz, J. A.; Elbert, S. T.; Gordon, M. S.; Jensen, J. H.; Koseki, S.; Matsunaga, N.; Nguyen, K. A.; Su, S.; Windus, T. L.; Dupuis, M.; Montgomery, J. A. *J. Comput. Chem.* **1993**, *14*, 1347–1363. (b) Gordon, M. S.; Schmidt, M. W. In *Theory and Applications of Computational Chemistry: The First Forty Years*; Dykstra, C. E., Frenking, G., Kim, K. S., Scuseria, G. E., Eds.; Elsevier: Amsterdam, 2005; pp 1167−1189.

(39) Check, C. E.; Faust, T. O.; Bailey, J. M.; Wright, B. J.; Gilbert, T. M.; Sunderlin, L. S. *J. Phys. Chem. A* **2001**, *105*, 8111–8116.

(40) (a) Feller, D. *J. Comput. Chem.* **1996**, *17*, 1571–1586. (b) Schuchardt, K. L.; Didier, B. T.; Elsethagen, T.; Sun, L.; Gurumoorthi, V.; Chase, J.; Li, J.; Windus, T. L. *J. Chem. Inf. Model.* **2007**, *47*, 1045–1052.

(41) CrysAlis CCD; Oxford Diffraction, Ltd.; Version 1.171.27p5 beta (release 01-04-2005, CrysAlis171.NET).

(42) CrysAlis Red; Oxford Diffraction, Ltd.; Version 1.171.27p5 beta (release 01-04-2005, CrysAlis171.NET).

(43) Altomare, A.; Cascarano, G.; Giacovazzo, C.; Guagliardi, A. *J. Appl. Crystallogr.* **1993**, *26*, 343–350.

(44) Sheldrick, G. M. *SHELXS-97, Program for the Solution of Crystal Structures*; University of Göttingen: Göttingen, Germany, 1997.

(45) Farrugia, L. J. *J. Appl. Crystallogr.* **1999**, *32*, 837−838.

(46) Spek, A. L. *PLATON, A Multipurpose Crystallographic Tool*; Utrecht, The Netherlands, 1999.